

Robot for Magnetic Resonance Imaging Guided Focal Prostate Laser Ablation¹

Alexander Squires

College of Engineering,
The University of Georgia,
Athens, GA 30602

Sheng Xu

Department of Radiology and Imaging Sciences,
Center for Interventional Oncology,
National Institutes of Health,
Bethesda, MD 20892

Reza Seifabadi

Department of Radiology and Imaging Sciences,
Center for Interventional Oncology,
National Institutes of Health,
Bethesda, MD 20892

Yue Chen

College of Engineering,
The University of Georgia,
Athens, GA 30602

Harsh Agarwal

Philips Research North America,
Briarcliff, NY 10510

Marcelino Bernardo

Department of Radiology and Imaging Sciences,
Center for Interventional Oncology,
National Institutes of Health,
Bethesda, MD 20892

Ayele Negussie

Department of Radiology and Imaging Sciences,
Center for Interventional Oncology,
National Institutes of Health,
Bethesda, MD 20892

Peter Pinto

Department of Radiology and Imaging Sciences,
Center for Interventional Oncology,
National Institutes of Health,
Bethesda, MD 20892

Peter Choyke

Department of Radiology and Imaging Sciences,
Center for Interventional Oncology,
National Institutes of Health,
Bethesda, MD 20892

Bradford Wood

Department of Radiology and Imaging Sciences,
Center for Interventional Oncology,

National Institutes of Health,
Bethesda, MD 20892

Zion Tsz Ho Tse

College of Engineering,
The University of Georgia,
Athens, GA 30602

1 Background

Approximately, 240,000 men in the U.S. are diagnosed with prostate cancer annually [1]. The majority of these cases represent low-risk, organ-confined disease for which targeted therapy has emerged as a treatment alternative that spares patients from undesired side effects such as impotence and incontinence [2]. Focal laser ablation (FLA) utilizes a diode laser catheter to generate a well-controlled ablation zone, causing rapid heating of targeted cancerous tissue, and leaving the majority of the surrounding gland intact. While FLA for localized prostate cancer is receiving increased attention due to its minimally invasive nature, the procedure has several technical limitations. Most notable are the difficulty of (1) effectively localizing the prostate tumor according to the treatment planning, (2) safely placing the laser catheter to ablate the entire tumor and achieve adequate margins, and (3) accurately monitoring the ablated area. Larger tumors require multiple catheter placements, which can be difficult to achieve in an accurate and repeatable manner using current free-hand/template-based techniques.

A carefully designed robotic system can simplify magnetic resonance imaging (MRI)-guided prostate therapy by:

- optimizing the access to the prostate target
- improving the positioning accuracy and repeatability
- reducing downtime between ablation and procedure time

In this paper, a robotic system for MRI-guided prostate FLA is presented. We hypothesized that accurate placement of laser catheters to planned tumor locations could be achieved under MRI guidance and robotic positioning, critically important to avoid unnecessary gland punctures as well as to ensure the ablation treatment covering full volume of the tumor. This would maximize the utility of a minimally invasive system. Preoperative parametric MRI information together with intraoperative magnetic resonance (MR) thermometry imaging could update the plan iteratively after each ablation [3].

2 Methods

2.1 Robotic Positioner. The goal of developing an MR-conditional robotic system imposes several limitations on the use of materials to be plastics and small amounts of nonferromagnetic metals for patient safety and preserving image quality. Spatial limitations imposed by the small cylindrical bore (55–70 cm) of an MRI scanner and workspace required by prostate targeting dictate the available volume for the robot to occupy and the volume over which the robot must provide targeting capabilities. The prostate targeting volume was determined to be an approximately 50 mm square region in the transverse plane; open space between the needle guide and the bore opening was needed to allow operation.

A slim robot design built around a Core-XY belt system was chosen as a solution to the design requirements (Fig. 1(a)). The Core-XY system utilizes a single belt, in which the targeting is controlled by two pneumatic motors to position the end effector of the robot. Each motor integrates a pair of fiber-optic lines, generating quadrature pulses for positional encoding with a resolution of 0.005 deg. The end effector movement (ΔX , ΔY) is related to the rotation of two motors (ΔA , ΔB) mathematically as follows:

¹Accepted and presented at The Design of Medical Devices Conference (DMD2016), April 11–14, 2016 Minneapolis, MN, USA.

DOI: 10.1115/1.4033805

Manuscript received March 1, 2016; final manuscript received March 17, 2016; published online August 1, 2016. Editor: William Durfee.

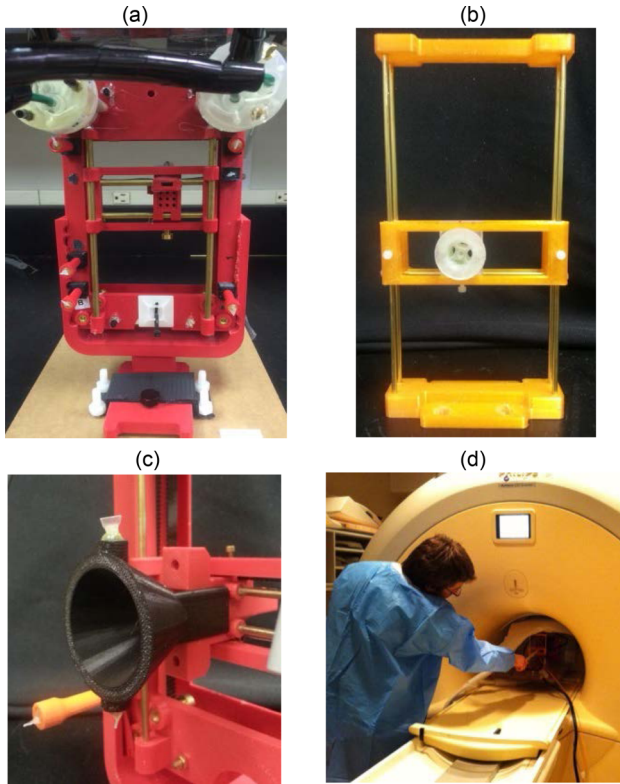


Fig. 1 Needle guidance robot and remote insertion. (a) Surgeon's view of the robot. (b) Manually aligned remote guide. (c) Alignment cone on needle guide. (d) Remote insertion of catheter with extension arm.

$$\Delta X = \frac{1}{2}(\Delta A + \Delta B) \quad (1)$$

$$\Delta Y = \frac{1}{2}(\Delta A - \Delta B) \quad (2)$$

$$\Delta X + \Delta Y = \Delta A = \frac{n_{\text{pulses},A}}{4} (2\pi r_{\text{pulley}}) \quad (3)$$

$$n_{\text{pulses},A} = 2 \frac{\Delta A}{\pi r_{\text{pulley}}} \quad (4)$$

The robot registration to the MRI coordinate system was achieved using five gadolinium fiducial markers (PinPoint, Beekley, Inc., Bristol, CT) mounted on the robot. This robot was designed for use in conjunction with Visualase[®] laser ablation catheter kits and its laser generator.

2.2 Remote Insertion. A remote insertion guide (Fig. 1(b)) placed proximal to the surgeon allowed the user standing at the bore opening to insert the catheter under real-time MRI guidance and without needing to remove the patient from the bore. After positioning the needle guide, the remote insertion guide was aligned manually with the robot by the surgeon, and the catheter was inserted through the guide toward the robot. The alignment cone (Fig. 1(c)) corrected any misalignment caused by the distance between the robot and the remote insertion guide by channeling the inserted catheter to the end effector needle guide.

2.3 Software and Control. A LabVIEW[™] (National Instruments, Austin, TX) GUI displayed the workspace, end effector position, and controlled target position. Operators could choose to drive the end effector to the target position themselves or via

automatic control. Targeting control was performed using a positioning-seeking algorithm. Based on the known change in desired position, the necessary changes in the rotational positions of the motors were calculated. Using the optical encoder pulse count, the target motor position was updated relative to the current position. Pneumatic motor control was implemented using proportional-integral-derivative (PID) modulated pulse-width modulation (PWM) compressed air supply.

2.4 Accuracy and Efficacy Testing. Full system tests were performed in a clinical Philips Achieva 3.0T TX MRI system at the National Institutes of Health Clinical Center in order to quantify MRI compatibility, insertion accuracy, and streamline operational workflow, as reported in Sec. 3. The workflow was designed to reduce the time spent compared to traditional FLA procedures done under MR guidance.

3 Results

3.1 MRI Compatibility. The signal-to-noise (SNR) ratios of MR images in a homogenous phantom filled with CuO₄ diluted saline were calculated in the conditions with the robot (1) absent, (2) present, and (3) moving, respectively, to qualify the MRI compatibility of the robot. The maximum SNR variation was < 7.5%, falling within an acceptable range for devices used inside MRI.

3.2 Accuracy Validated in MRI. Insertion accuracy tests were carried out at NIH utilizing a prostate phantom to perform brachytherapy seed placement (Figs. 2(a)–2(d)). The positioning errors of the seed placements ($n=10$) were $\mu=0.9$ mm and

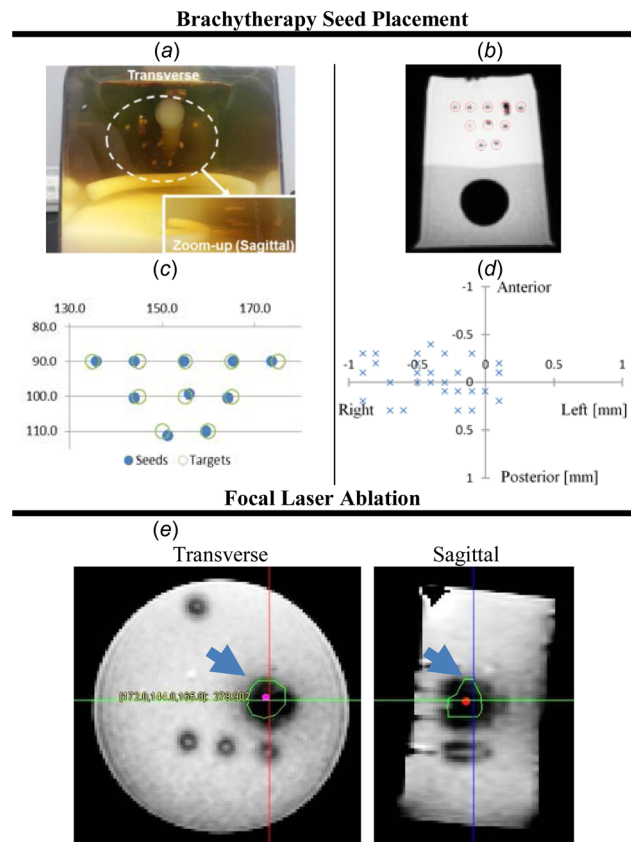


Fig. 2 ((a)–(d)) Brachytherapy seed placements and error quantifications: (a) seeds in prostate phantom, (b) MR images, (c) targets and seeds overlaid (mm), and (d) positioning error map. (e) FLA showing darker ablated zones and virtual tumor outline (indicated by arrow); mild overtreatment is acceptable.

$\sigma = 0.4$ mm perpendicular to the insertion axis, and $\mu = 1.9$ mm and $\sigma = 2.7$ mm along the insertion axis. These errors were calculated from a volumetric scan with perpendicular error being calculated from pixels of 1.18 mm per side and insertion error from image slices 3.5 mm thick.

3.3 System Efficacy. Measurements of catheter insertion accuracy were performed in anatomical prostate phantoms with physical tumors ($n = 5$) and temperature-sensitive phantoms with virtual tumors ($n = 8$). Insertion accuracy of the catheter relative to the designated target point was under 2 mm ($\mu = 1.7$ mm and $\sigma = 0.2$ mm). Analysis of the ablated regions (Fig. 2(e)) demonstrated that 100% of the tumor volume was treated in each case. Operation time, including setup, was 60 min plus 10 min per ablation.

4 Interpretation

The needle guidance robot and remote insertion system were tested as assistive technologies for MR imaging-guided and thermometry monitored laser ablations. Robot-assisted MRI-guided

FLA demonstrates promise by providing accuracy at clinically relevant levels while supplying the ability to perform manually driven remote insertions. Accurate ablation of the target tumor volumes was performed according to the treatment plan, preserving the surrounding tissue regions. Future work includes in vivo animal and human studies to validate the accuracy and efficiency of the needle guidance robot and the treatment planning software for effective MRI-guided FLA treatment.

References

- [1] Siegel, R., Ma, J., Zou, Z., and Jemal, A., 2014, "Cancer Statistics, 2014," *CA-Cancer J. Clin.*, **64**(1), pp. 9–29.
- [2] Raz, O., Haider, M. A., Davidson, S. R., Lindner, U., Hlasny, E., Weersink, R., Gertner, M. R., Kucharczyk, W., McCluskey, S. A., and Trachtenberg, J., 2010, "Real-Time Magnetic Resonance Imaging-Guided Focal Laser Therapy in Patients With Low-Risk Prostate Cancer," *Eur. Urol.*, **58**(1), pp. 173–177.
- [3] Xu, S., Kruecker, J., Amalou, H., Kwak, J. T., and Wood, B. J., 2014, "Real-Time Treatment Iterative Planning for Composite Ablations," *Computer Assisted Radiology and Surgery 28th International Congress and Exhibition (CARS 2014)*, Fukuoka, Japan, June 25–28, pp. 52–53.